# Phase transitions in load transfer models of fracture

Y. Moreno[a,b,*], J.B. Gómez[c], A.F. Pacheco[b]

[a] *The Abdus Salam International Centre for Theoretical Physics, P.O. Box 586, Strada Costiera 11, Trieste I34100, Italy*
[b] *Departamento de Física Teórica, Universidad de Zaragoza, Zaragoza 50009, Spain*
[c] *Departamento de Ciencias de la Tierra, Universidad de Zaragoza, Zaragoza 50009, Spain*

## Abstract

The possible parallelism existing between phase transitions and fracture in disordered materials is discussed using the well-known fiber bundle models and a probabilistic approach suited to smooth fluctuations near the critical point. Two limiting cases of load redistribution are analyzed: the global transfer scheme, and the local transfer rule. The models are then studied and contrasted by defining the branching ratio as an order parameter indicative of the distance of the system to the critical point. In the case of long range interactions, i.e., the global rule, the results indicate that fracture can be seen as a second-order phase transition, whereas for the case of short range interactions (the local transfer rule) the bundle fails suddenly with no prior significant precursory activity signaling the imminent collapse of the system, this case being a first-order like phase transition. © 2001 Elsevier Science B.V. All rights reserved.

*Keywords:* Criticality; Fibre bundle model; Phase transitions

## 1. Introduction

Fracture phenomena have attracted a lot of interest in the last several years, both experimentally and theoretically. In the lab, a disordered material subjected to an increasing external load can be experimentally studied by measuring the acoustic emissions before the global rupture. It has been shown [1,2] that this intense precursory activity in the form of bursts of different microscopic sizes follows a well-defined

* Corresponding author. The Abdus Salam International Centre for Theoretical Physics, P.O. Box 586, Strada Costiera 11, Trieste I34100, Italy.
*E-mail address:* yamir@ictp.trieste.it (Y. Moreno).

power law. From the theory side, the understanding of fracture in heterogeneous materials has progressed due to the use of lattice models and large scale numerical simulations [3]. Recently, the introduction of models of material failure has led to the evidence that rupture can be viewed as a kind of critical phenomenon [3–8]. Nevertheless, the question of whether rupture exhibits the properties of a first-order or a second-order phase transition remains under discussion as well as what is the order parameter that determines the type of transition.

In this field, it is important to use models that are able to describe the complexity of the rupture process, although they should be simple enough to permit analytical insights. To this class of models belong the well-known fiber bundle models (FBM) widely used since their introduction more than 40 years ago [9,10]. In static FBM, a set of fibers (elements) is located on a supporting lattice and one assigns to its elements a random strength threshold sampled from a probability distribution. The lattice is loaded and fibers break if their loads exceed their threshold values. Now, one can assume different load transfer rules to mimic the range of interactions among the fibers in the set. The global load sharing rule is the simplest theoretical approach one can adopt to make the problem analytically tractable, which implies that the load carried by failed elements is equally distributed among the surviving elements of the system, representing in this way a long range interaction among the constituent parts of the system. This is a kind of mean field approach to the more extreme local load sharing scheme, where the interaction among the elements is short range and the load supported by the failing elements is transferred only to a neighborhood.

Very recently [11], we have developed a probabilistic approach suited to smoothen the fluctuations around the point of final collapse. In this paper, we extend the method to analyze the local load sharing scheme and contrast the two limiting cases of range interactions: the long range and the short range. While for the case of global load sharing, we obtain different scaling relations that point out that the fracture of a fiber set with long range interactions may be a continuous transition, for the case of short range interactions, the failure exhibits no significant precursory activity and the system breaks abruptly showing, in this case, the properties of a first-order transition where no scaling laws can be identified. The rest of the paper is organized as follows. In Section 2, we present the standard approach to the FBM. In Section 3, we introduce the new probabilistic method and the results derived from it and from Monte Carlo simulations. Finally, Section 4 is devoted to discussion and conclusions.

## 2. Static fiber bundle models

Let us first recall the basic ingredients of the static FBM and how one proceeds in numerical simulations. The term static means that time plays no role in the model [12]. The system under consideration is a set of $N_0$ elements (fibers) located in a supporting lattice each one having at the initial state a zero load and a *fixed* strength threshold value (quenched disorder) sampled randomly from a probability distribution $P(\sigma)$. The

system is then subjected to an external force $F$ which is shared democratically among the fibers, that is, the distribution of the total force produces that each element increases it load, $\sigma$, in the same amount. This individual stress acts as the control parameter. The loading process is done quasistatically, i.e., the external force is increased at a sufficiently slow rate so as to produce a single breaking event when the stress in the weakest element equals its threshold value. Then, the increase of external force stops and the load of the broken fiber is transferred according to the transfer scheme assumed. In the global load sharing FBM, this implies that the load on fiber $i$ is given by $\sigma_i = F/n_s(F)$, where $n_s$ is the number of surviving elements for a given external load $F$. In the local load sharing FBM, the above relation does not hold any more because there the redistribution of load is performed among the nearest neighbors of the failed fiber giving rise to the appearance of regions with different stress concentrations.

In both schemes, the rupture of a fiber may induce secondary failures which in turn may trigger more failures. This process of induced failure at constant external load, termed avalanche, stops when all surviving elements carry a load lower than their thresholds. The system is then loaded again and the process is repeated until the final catastrophic avalanche provokes the total rupture of the material, which occurs at a critical load $\sigma_c$ that depends on the probability distribution from where the individual strengths were drawn as well as on the system size. At this point, it is worth recalling that the exact value of $\sigma_c$ can be analytically obtained in the thermodynamic limit for the global load sharing case while for local load sharing schemes there is no theoretical approach leading to $\sigma_c$. It is also known that the critical load $\sigma_c$ for the global load sharing FMB is non-zero and independent of $N_0$ for $N_0 \to \infty$, whereas $\sigma_c$ tends to zero as $N_0$ goes to infinity in the case of local load sharing models [10,13]. Fiber bundle models have also been recently used in self-organized criticality (SOC), a theoretical framework widely used for the study of avalanche phenomena in disordered systems. It has been shown using these models that systems with plastic behavior can reach a SOC state just before the global rupture [14]. A second case of self-organization with power law distributions in several quantities corresponds to the situation in which the fracture process coexists with a healing process [15].

In numerical simulations, the cycle of complete breakdown of the material is performed many times in order to average out the effect of fluctuations. Nevertheless, the stress history of a particular element is made of steps, so that the fluctuations around the critical load can never be completely avoided. Let fiber $k$ be supporting a stress $\sigma_k^0$ at a given step of the failure process. It will continue to support $\sigma_k^0$ until a global driving or a stress transfer from one (or more) of the failed elements occurs. At this moment, element $k$ instantaneously changes its load to $\sigma_k^1 = \sigma_k^0 + \sigma_{dist}$, where $\sigma_{dist}$ is the load coming from the failed fibers or from the global driving. So, in a later step, element $k$ could receive again load, suffering a second step-like increase in stress. This step-like stress history continues until fiber $k$ fails. As we are interested in studying the behavior of the system as the critical point is approached, it is of utmost importance to find a simple method that is able to capture the evolution of the system near the critical point avoiding as much as possible the fluctuations.

## 3. Probabilistic approach to static fiber bundle models

Let there be a set of $N_0$ elements located on a supporting lattice. Suppose that each element carries a given load $\sigma$, which is set to zero at the initial state. Fibers break depending on their strengths which are distributed according to a probability distribution $P(\sigma)$. Different probability distributions can be considered. In materials science the Weibull distribution is widely used,

$$P(\sigma) = 1 - e^{-(\sigma/\sigma_0)^\rho} , \tag{1}$$

where $\rho$ is the so-called Weibull index, which controls the degree of disorder in the system (the bigger the Weibull index, the smaller the disorder), and $\sigma_0$ is a load of reference. In the following, we will assume $\sigma_0 = 1$, and therefore, the loads are dimensionless. Although the results we show hereafter are for the Weibull distribution to gain in definiteness, they have been also obtained for a wide class of distributions. Besides, for continuous distributions decaying fast enough, the approach to the critical state does not depend on the detailed form of the disorder [16].

Eq. (1) represents the probability that an element fails under the individual load $\sigma$. Now, consider the case in which an element drawn from Eq. (1) supports a load $\sigma_1$, but breaks under a new load $\sigma_2$. The probability that this happens is given by

$$p(\sigma_1, \sigma_2) = \frac{P(\sigma_2) - P(\sigma_1)}{1 - P(\sigma_1)} , \tag{2}$$

which is equal to

$$p(\sigma_1, \sigma_2) = 1 - e^{-(\sigma_2^\rho - \sigma_1^\rho)} . \tag{3}$$

So, the probability $q(\sigma_1, \sigma_2)$ that an element that has survived to the load $\sigma_1$ also survives to the load $\sigma_2$ will be given by

$$q(\sigma_1, \sigma_2) = 1 - p(\sigma_1, \sigma_2) = e^{-(\sigma_2^\rho - \sigma_1^\rho)} . \tag{4}$$

All these probabilities depend on the state of stress of each element, which is a complex function of both the control parameter and the stress redistributions due to fiber failures. To mimic the quasistatic increase in load on the system as is applied in MC simulations, we impose the condition that under an external force $F$, the next breaking event consists of one single failure. Now, we will explore how the driving process controls the approach to global failure in the global load sharing case and in a particular version of the local load sharing schemes.

### 3.1. Global load sharing case

Let us suppose that after the latest avalanche, there are $N_k$ surviving elements each one bearing a load $\sigma_k$. The assumption of quasistatic increase in load on the system

implies that the load $\sigma_l$ needed to provoke the failure of only one element is [11]

$$\sigma_l = \left[ \sigma_k^\rho - \ln\left( 1 - \frac{1}{N_k} \right) \right]^{1/\rho} , \tag{5}$$

where in Eq. (5) $N_k = N_0$ and $\sigma_k = 0$ at the initial state. Elevating the external force up to the $N_k \sigma_l$ level, a first element breaks. As we are dealing with a global load sharing set, the choice of the broken element is irrelevant because all of them are equivalent. Once the first element fails, the redistribution of its stress takes place which may induce secondary failures and so on, until the end of the avalanche.

Now, the number of surviving elements in the set after an avalanche has come to an end can be calculated by the recursive relations [11],

$$N_{j+1} = N_j q(\sigma_{j-1}, \sigma_j) , \tag{6}$$

$$N_j \sigma_j = N_{j-1} \sigma_{j-1} , \tag{7}$$

$$N_j = N_{j+1} . \tag{8}$$

Eq. (6) relates the number of surviving elements between two successive avalanche steps, whereas Eq. (7) allows the computation of the new load acting on the $N_j$ surviving elements. This is possible because we are under a global load sharing scheme and thus all surviving elements support the same load. Finally, Eq. (8) determines the end of the ongoing avalanche.

The dynamics of the system is completely determined by Eqs. (5)–(7). In this way, the size of an avalanche is given by the number of elements that break between two successive steps of external loading. The total stress accumulated in the system can be calculated multiplying the number of intact fibers before an avalanche starts by the load given by Eq. (5). The critical load, defined as the load needed to provoke the total collapse of the system, is equal to the load on the intact fibers just before the final catastrophic avalanche. Note that in this probabilistic approach, in contrast to Monte Carlo simulations, we need to store only the information concerning the loads of the intact elements, that is, the threshold dynamics is omitted with the subsequent advantages of saving computer resources and the possibility of exploring systems of larger size.

For Eq. (8) to be satisfied, we can proceed in two different ways in order to determine when an avalanche ends, to which we will refer to as the continuous and the discrete cases. For the continuous case, the number $N_{j+1}$ of surviving elements is considered a real number. This means that condition (8) is never fulfilled before the final avalanche. So, condition (8) is replaced in numerical simulations by a factor $v \ll 1$ that determines the end of an avalanche, i.e., if $N_j - N_{j+1} \leqslant v$ the avalanche stops; otherwise it continues. In the discrete case, $N_{j+1}$ is considered to be an integer number, so that after each iteration of Eq. (6), $N_{j+1}$ has to be rounded up. This is done comparing the remainder of $N_{j+1}$, $\lambda$, with a random number $\alpha$ uniformly distributed in the interval $[0, 1[$. Thus, if $\alpha \geqslant \lambda$, $N_{j+1}$ is equal to its whole part, and if not, $N_{j+1}$
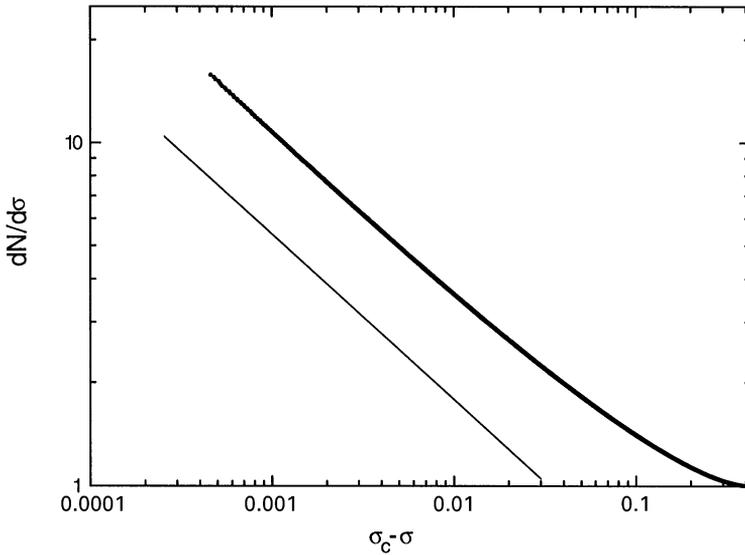
Fig. 1. Rate of fiber failure as a function of the distance to the critical point for the continuous version of the probabilistic global load sharing model for a system of $N_0 = 50\,000$ elements and $\rho = 2$. A line with the mean-field value $\gamma = \frac{1}{2}$ of the exponent is plotted for reference.

is equal to its whole part plus one. Next, we check whether condition (8) is satisfied for the rounded value of $N_{j+1}$ or if a new iteration of Eq. (6) has to be performed. The continuous approach has the great advantage that the fluctuations are ruled out, whereas for the discrete case the results are similar to those obtained by Monte Carlo simulations where it is necessary to average over many realizations in order to get accurate mean values. This is because in the global fiber bundle model the central limit theorem applies [17,18].

Now, we proceed to explore the behavior of the system near the critical point. In particular, we are interested in inspecting the evolution of some quantities as the critical point is reached. In order to avoid unnecessary fluctuations around the critical point, the results shown below have been obtained for the continuous case of the probabilistic approach ($\rho = 2$). It turns out [11] that the avalanche size close to the critical point diverges with an exponent $\gamma = \frac{1}{2}$ as $s \sim (\sigma_c - \sigma)^{-\gamma}$. A similar behavior, through a mapping of a fuse network model to the global fiber bundle model used here, has been recently reported [6,7]. This mapping between fiber bundle models and fuse networks with strong disorder was first noted [19] a few years ago; nevertheless, it has also been pointed out that 3D fuse networks apparently do not follow the FBM picture [20]. Note, additionally, that for the probabilistic continuous version, this relation is obtained for a single realization avoiding, in this way, the large number of iterations performed in MC simulations. In Fig. 1 we have depicted the derivative of the number of broken fibers, ($dN/d\sigma$), as a function of the distance to the critical point $\sigma_c - \sigma$ in a log–log plot. This rate $dN/d\sigma$ diverges as $(\sigma_c - \sigma)^{-\gamma}$ also with $\gamma = \frac{1}{2}$, thus qualifying a

critical mean field behavior as was already shown [8] by means of analytical analysis of fiber bundle models. In Ref. [14], a similar scaling behavior is addressed for the derivative of the strain carried by the fibers with respect to the driving force.

Another way to shed light on the critical behavior of this type of system is to define a branching ratio $\zeta$ for each avalanche. This magnitude represents the probability to trigger future breaking events given an initial individual failure [21,22] and is related to the number of broken fibers by

$$\zeta = \frac{\langle z \rangle - 1}{\langle z \rangle} \ . \tag{9}$$

The above relation can be obtained by thinking of the evolution of fracture as a kind of branching process [23]. In this process, each node gives rise to a number $n$ of new branches in the next time step. The average number $\langle n \rangle$ of new branches is called the branching ratio. Let us denote by $n_t$ the number of branches at a given step $t$ of the branching process, and by $t_{max}$ the total number of time steps before it dies. Then,

$$\zeta = \langle n \rangle = \frac{\sum_{t=0}^{t_{max}-1} n_{t+1}}{\sum_{t=0}^{t_{max}} n_t} \ ,$$

and

$$\zeta = 1 - \frac{n_0}{\sum_{t=0}^{t_{max}} n_t} \ .$$

As $n_0 = 1$, $\zeta = 1 - (1/n_{tot})$ where $n_{tot}$ is the total number of nodes developed in the branching process. For a fracture process, $n_{tot}$ is equal to average number of failure events. So, Eq. (9) defines the branching ratio. We represent by $\langle z \rangle$ the average number of elements that fail in one avalanche, which is a function of the control parameter $\sigma$ and coincides with $s$. This analogy between fracture and branching processes has been previously used to study the criticality in the process of fragmentation of Hg drops [24]. The branching ratio will then act as the order parameter. It takes the value 1 when the system is critical, thereby representing a measure of the distance of the system from the critical state [22]. We would like to remark here two characteristics of the branching ratio defined as above. First, it coincides with its general definition for a branching process. Here, the values of the branching ratio are always less than or equal to one because we are analyzing an irreversible breaking process that cannot continue forever, so that a value of the branching ratio greater than one would imply a physically unreachable situation. Secondly, we have introduced a definition in terms of the *avalanche size* and not in terms of the *cluster size*. The avalanche size in fiber bundle models is a measure of *causally* connected broken sites while the cluster size is a measure of *spatially* connected broken sites. It is clear that in the global fiber bundle model, the spatial correlations are ruled out and then the distribution of avalanche sizes does not coincide with the distribution of cluster sizes.

We have numerically computed $\zeta$ for the continuous version of the probabilistic model. The results obtained for a system of $N_0 = 50\,000$ elements and $\rho = 2$ have been
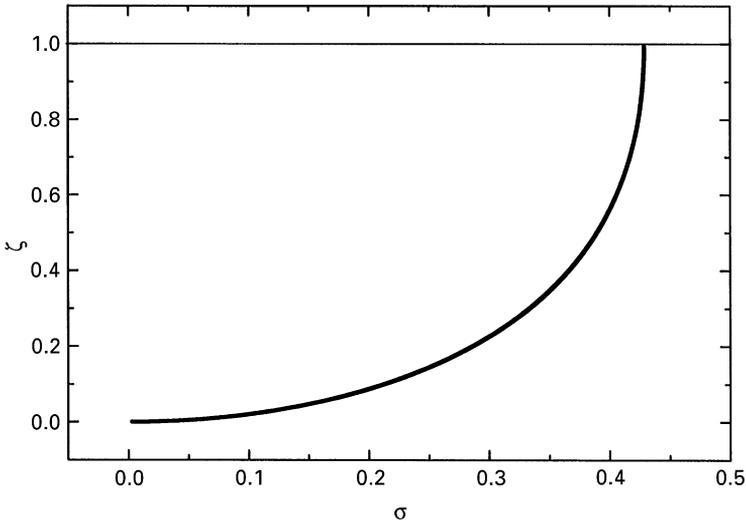
Fig. 2. Evolution of the branching ratio as the critical point is approached in the continuous probabilistic method ($N_0 = 50\,000$). Note that at the critical point the branching ratio reaches the unity.
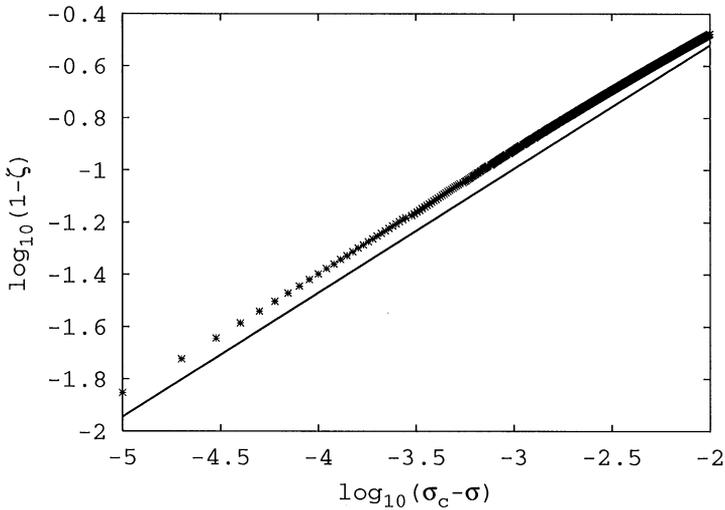


Fig. 3. Behavior of the branching ratio near the critical point. The straight line satisfies relation $(1 - \zeta) \sim (\sigma_c - \sigma)^{\beta}$, with $\beta = 0.5$. This plot has been obtained for a uniform distribution of fiber's strengths.

plotted in Fig. 2. It can be seen in this figure that the branching ratio approaches the unity as the critical load is reached. In the figure, the values of $\zeta$ are collected for all the avalanches except for that which provokes the catastrophic event leading to the collapse of the system. So, this dependency of $\zeta$ with $\sigma$ means that very close to the critical point, the initial failure provokes the breaking of another fiber which in turn induces tertiary ruptures and so on. This is the result that should be expected from the divergence of the avalanche size at the critical point. Fig. 3 shows the behavior
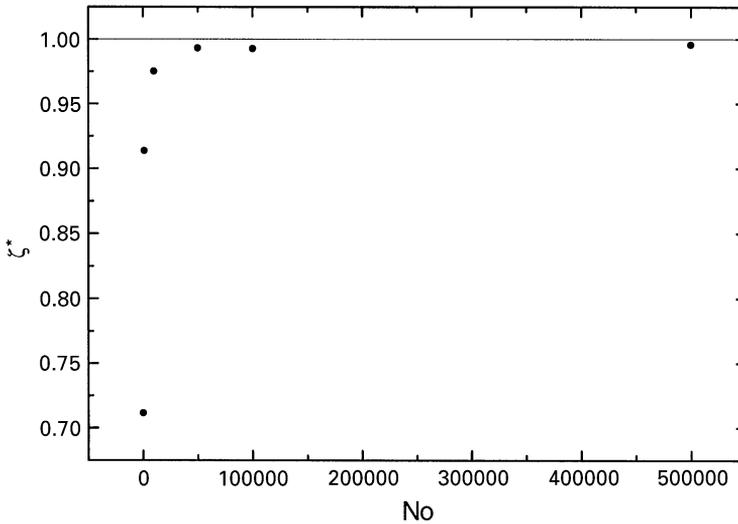
Fig. 4. Branching ratio for different system sizes ($\rho = 2$) for the global load sharing case. As the size of the system is increased the value of the branching ratio for the last non-catastrophic avalanche approaches unity.

of the order parameter near the critical point. As can be seen, near the critical point, the relation $1 - \zeta \sim (\sigma_c - \sigma)^\beta$, where $\beta = \frac{1}{2}$ applies. Note the similarity of the behavior with those obtained for the magnetization in known magnetic systems with second-order phase transitions. It is of additional interest to note that the branching ratio also captures the feature that the precursory activity is significant only for strong disorder (for the Weibull distribution, small values of $\rho$); whereas for small disorder the system behaves more similar to the breakdown of homogeneous materials. On the other hand, the branching ratio does not depend on the size of the system for large systems, in contrast to previous results in other fracturing systems [22]. In Fig. 4 we illustrate this behavior by plotting the value of the branching ratio for the last non-catastrophic avalanche, $\zeta^*$, as a function of the system size. In all cases, the numerical simulations were performed for $\rho = 2$. It is clear from the figure that $\zeta^*$ reaches the unity as $N_0$ goes to infinity.

## 3.2. Local load sharing case

It is well-known that the local load sharing FBM is much more complicated than the global load sharing case. The complexity of the fracture problem increase because the load borne by failed elements is transferred to nearest neighbors and then there appear regions of stress concentration throughout the system. The distribution of load is now not homogeneous, and we have to carry on several lists to record the individual load of the fibers in the system. However, with the probabilistic approach, we are able to study a few things about the behavior of the system, which are sufficient to remark the great differences between the long range and the short range interactions schemes.

One important difference between the two schemes is that contrary to the global load sharing case, in the local scheme there is no significant precursory activity signaling the approach to the final collapse and the system undergoes an abrupt catastrophic avalanche. For maximum simplicity, we consider next a one-dimensional periodic local load system where the stress transfer is done by adding the load of the failed element always to the element on its right. Despite its simplicity, it has been shown [25] that the general properties of this particular model are identical to those of more complex local schemes.

The probability that the system fails in only one avalanche is given by

$$p(\sigma_1, \sigma_2)\,p(\sigma_1, \sigma_3)\,p(\sigma_1, \sigma_4)\ldots p(\sigma_1, \sigma_{N_0}),\tag{10}$$

where $\sigma_i = i\sigma_1$ and $\sigma_1$ is

$$\sigma_1 = \left(0 - \ln\left(1 - \frac{1}{N_0}\right)\right)^{1/\rho}.$$

That is, the probability of having a one-step failure is given by the probability that an element fails under a load $\sigma_2$ having survived to the load $\sigma_1$, multiplied by the probability that the next element in the lattice also fails under the new load $\sigma_3$ having survived to the load $\sigma_1$ and so on.

On the other hand, Eq. (4) takes the form

$$q(i,j) = e^{-\sigma_1^\rho(j^\rho - i^\rho)},\tag{11}$$

which gives the probability that an element that has survived to the load $i\sigma_1$ also survives to a new load $j\sigma_1$, being $\sigma_1$ the load that produces the first breaking event in the system at the initial state. The probability that the first avalanche consists of, for example in one failure, is given by $q(1,2)$. The first avalanche will have size two with probability $p(1,2)q(1,3)$. In general, the probability that the first avalanche does not provoke the rupture of the whole system, i.e., be finite, is given by

$$P_1 = \sum_{l=1}^{\infty} \Pi_l q(1, l+1),\tag{12}$$

where

$$\Pi_l = p(1,2)\,p(1,3)\ldots p(1,l) = \prod_{i=2}^{l} p(1,i), \quad l < N_0,$$

with $\Pi_1 = 1$. Thus, the average size of the first avalanche, derived from Eq. (12) is

$$S_1 = \sum_{l=1}^{\infty} l\,\Pi_l q(1, l+1).\tag{13}$$

Numerical simulations of the continuous case, the discrete approximation (both defined as above for the global load sharing scheme) and Monte Carlo method confirm the validity of Eq. (13). For example, for $\rho = 2$ and $N_0 = 1000$ we obtain $S_1 = 1.0030$, $S_1 = 1.0022$ and $S_1 = 1.0039$, respectively. This result is valid only for the first avalanche in the system.

We have also verified by means of Monte Carlo simulations that for this local transfer rule, there is no power law in the distribution of avalanche sizes. Besides, no scaling relations appear and the system is more sensitive to parameters such as the degree of disorder ($\rho$) and the size of the system $N_0$. Catastrophic avalanches arise very often in the first stages of the rupture process.

Finally, we illustrate how one can describe the precursory activity when it is limited to a few steps before the global rupture. Let us solve the particular situation in which the first avalanche is finite and the second provokes the final breakdown of the system. The load needed to break the first element at the initial state is

$$\sigma_1 = \left( -\ln\left( 1 - \frac{1}{N_0} \right) \right)^{1/\rho} \simeq \left( \frac{1}{N_0} \right)^{1/\rho}, \quad N_0 \gg 1 .$$

So $\sigma_1^\rho \simeq 1/N_0$, and

$$q(1,2) = e^{-(2^\rho-1)1/N_0} . \tag{14}$$

If the value of $q(1,2)$ in Eq. (14) is bigger than 0.5, then the fracture will likely consist of one single event of rupture and the avalanche will not progress beyond this first failure. As shown above, for $\rho = 2$ a system size of $N_0 = 1000$ elements is enough to produce first avalanches of size 1 on average. Next, the driving force is increased and the new load acting on the surviving $N_0 - 1$ fibers is

$$\sigma_2 = \left( \sigma_1^\rho - \ln\left( 1 - \frac{1}{N_0 - 1} \right) \right)^{1/\rho} \simeq \left( \frac{2}{N_0} \right)^{1/\rho}, \quad N_0 - 1 \gg 1$$

that is, $\sigma_2^\rho = 2/N_0$. In the derivation of $\sigma_2$ it has been assumed that the second avalanche starts with high probability in a fiber different from that which is located just in the crack tip of the first avalanche. This approximation is well-justified by numerical simulations of this local load model for which it is known that the first breaking events are randomly distributed in the sample, leading to the appearance of several small cracks which much later coalesce and grow provoking the final breakdown. Now, there are $(N_0 - 2)$ elements bearing a load $\sigma_2$ and one element supporting a load $\sigma_2 + \sigma_1$. The system will experience on average the final breakdown in this second breaking event if the probability

$$q'(1,2) = e^{-(2^\rho-1)2/N_0} \tag{15}$$

is lower than 0.5. Nevertheless, $q(1,2)$ and $q'(1,2)$ are not independent since the relation

$$q'(1,2) = (q(1,2))^2 \tag{16}$$

has to be verified. This dependence, together with the restrictions $q(1,2) > 0.5$ and $q'(1,2) < 0.5$ leads to $0.5 < q(1,2) < 0.7$ and $0.25 < q'(1,2) < 0.5$ as acceptable values for $q(1,2)$ and $q'(1,2)$ in order to have a two-step system collapse. This approximation seems reasonable taking into account the way in which numerical simulations of the continuous and the discrete versions of the probabilistic approach proceed. So,

the condition for the first avalanche to be finite and that the second breaks the system is reduced to

$$N_0 \simeq 2^{\rho+1} - 2 \tag{17}$$

for $q(1,2) = 0.6$, a value in the middle of its range. This relationship between $N_0$ and $\rho$ is confirmed in numerical simulations. The situation considered above corresponds to a very brittle rupture since the ratio of the size of the typical local damage that induces the system failure to the system size is very close to one $(N_0 - 1)/N_0$. Expression (17), although very simple, gives a rough estimate of the qualitative relation between the size of the system and the amount of disorder when the degree of brittleness of the fracture is high. The situation analyzed becomes important and more accurate as we go to larger system sizes because for the local load transfer rule and a larger number $N$ of fibers, the probability to find a weak region somewhere in the system is high and due to the local redistribution rule, the crack will propagate fast enough to break the whole system in a few steps (strictly speaking, in the thermodynamic limit the critical load is zero).

## 4. Discussion and conclusions

We have proposed a probabilistic approach to fiber bundle models of fracture. The cases of long range interactions among the fibers of the bundle and a local load sharing transfer scheme (short range interactions) were considered in order to investigate the behavior of the system near the global breakdown of the material. The results obtained for the local scheme indicate that the system undergoes a kind of first-order phase transition in agreement with previous reports [6,7,26]. The system fails with no significant precursors announcing the incipient rupture, and no scaling relations can be found even for large system sizes and strong disorder. We illustrated this behavior by considering the situation of a two-step global failure. In this particular case, several quantities have a discrete jump at the critical point, like the branching ratio $\zeta$ which goes from zero to $(N_0 - 2)/N_0 - 1$, i.e., from zero to one in the limit of $N_0 \to \infty$.

The scenario is quite different for the global load sharing FMB. In this case, the type of phase transition is not very clear. There are basically two possible ways in which such a transition may occur. In a first-order phase transition, we find discontinuous behavior in various quantities as we pass through the critical point. Contrary to this case, in a second-order (or continuous) phase transition, the fluctuations are correlated over all length scales, therefore, not only does the correlation length diverges continuously as the critical point is approached, but also other quantities show scaling [27]. A particular case is the first-order phase transition close to a spinodal-like instability, for which scaling relations can be obtained despite that some macroscopic quantities, like the elastic modulus, have a discrete, finite jump at the critical point [28]. The question then is whether the global load sharing FBM is a case of a second-order transition or a first-order spinodal transition.
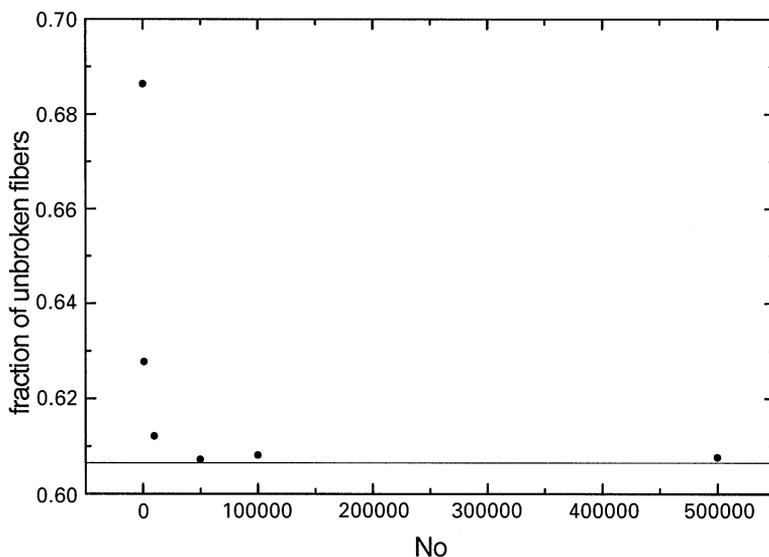
Fig. 5. Fraction of unbroken fibers just before the final breakdown in the probablistic model of the global load sharing case as a function of the system size ($\rho = 2$). The horizontal line shows the exact value in the thermodynamic limit.

The results obtained with the probabilistic approach seem not to support the claim of Ref. [5] that the failure of a fiber bundle model under a global load sharing transfer scheme behaves as a first-order phase transition close to a spinodal point. There, by simulating models of electric breakdown and fracture, the authors presented ample numerical and theoretical evidence of several scaling relations and of the discrete jump of the macroscopic properties. We have obtained the same scaling relation for the rate of fiber failures as the critical point is reached, as well as for the avalanche sizes, which also diverge at the transition. Note that the scaling exponent derived from numerical simulations of the continuous version of the probabilistic approach fits very well the mean field result $\gamma = \frac{1}{2}$. Besides, the fraction of unbroken fibers just before the global rupture has a discontinuity, which is not size dependent for big systems as can be observed in Fig. 5. It has also been shown by analytic means that the distribution of avalanche sizes in the case of global load sharing transfer rule follows a universal power law with an exponent $-\frac{5}{2}$ [29–32].

However, we should notice that in driven disordered systems, the concepts related to spinodal nucleation are not sufficiently well-established. In particular, it seems that the finite size of the system makes it possible that the last catastrophic avalanche provokes the elastic modulus to drop to zero with a finite, and very likely, N-dependent jump. Thus, from our point of view, it is not enough to set the conclusion that fracture can be described as a first-order phase transition.

Our alternative point of view is to consider the *branching ratio* defined previously as a measure of the distance of the system from the critical point. According to the

results obtained, the branching ratio goes *continuously* from zero to one. The branching ratio measures the probability that a fiber that has failed triggers none, one or more breaking events. Therefore, a branching ratio equal to one at the critical point implies that, on average, one failure will induce another failure so that the system reaches a state where any perturbation propagates across the entire system, which is, in essence, a critical phase. This invokes a continuous phase transition as claimed in other analysis of fracture models [33]. Note, additionally, that what changes discontinuously at $\sigma_c$ is the rate of change of $\zeta$ rather than $\zeta$ itself.

In summary, we have introduced a probabilistic approach to fiber bundle models which allows to avoid the fluctuations near the critical point. The different rupture behaviours of the system for the global load sharing scheme and the local one were shown. For the short range interactions case, the rupture is no-doubt of the first-order phase transition type. For the global transfer rule, several scaling relations were obtained with mean field critical exponents. The branching ratio was defined as an appropriate order parameter. According to the results obtained, the branching ratio goes continuously from zero to one. This suggests that fracture in heterogeneous systems with long range interactions can be described as a phase transition of the second-order type, at least within the FBM picture.

## Acknowledgements

## References

[1] A. Garciamartin, A. Guarino, L. Bellon, S. Ciliberto, Phys. Rev. Lett. 79 (1997) 3202.
[2] A. Petri, G. Paparo, A. Vespignani, A. Alippi, M. Constantini, Phys. Rev. Lett. 73 (1994) 3423.
[3] K. Chakrabarti, L.G. Benguigui (Eds.), Statistical Physics of Fracture and Breakdown in Disordered Systems, Clarendon Press, Oxford, 1997, and references therein.
[4] H.J. Herrman, S. Roux (Eds.), Statistical Models for the Fracture of Disordered Media, North-Holland, Amsterdam, 1990.
[5] M. Sahimi, Phys. Rep. 306 (1998) 213, and references therein.
[6] S. Zapperi, P. Ray, H.E. Stanley, A. Vespignani, Phys. Rev. Lett. 78 (1997) 1408.
[7] S. Zapperi, P. Ray, H.E. Stanley, A. Vespignani, Phys. Rev. E 59 (1999) 5049.
[8] J.V. Andersen, D. Sornette, K.-T. Leung, Phys. Rev. Lett. 78 (1997) 2140.
[9] B.D. Coleman, J. Appl. Phys. 29 (1958) 968.
[10] H.E. Daniels, Proc. Roy. Soc. A 183 (1945) 404.
[11] Y. Moreno, J.B. Gómez, A.F. Pacheco, Phys. Rev. Lett. 85 (2000) 2865.
[12] M. Vazquez-Prada, J.B. Gomez, Y. Moreno, A.F. Pacheco, Phys. Rev. E 60 (1999) 2581, and references therein.
[13] D.G. Harlow, S.L. Phoenix, J. Composite Mater. 12 (1978) 195.
[14] F. Kun, S. Zapperi, H.J. Herrmann, Eur. Phys. J. B 17 (2000) 269.

[15] Y. Moreno, J.B. Gómez, A.F. Pacheco, Physica A 274 (1999) 400.
[16] R. da Silveira, Phys. Rev. Lett. 80 (1998) 3157.
[17] D. Sornette, J. Phys. A 22 (1989) L243.
[18] J. Galambos, The Asymptotic Theory of Extreme Order Statistics, New York, Wiley, 1978.
[19] A. Hansen, P.C. Hemmer, Phys. Lett. A 184 (1994) 394.
[20] V.I. Räisänen, M.J. Alava, R.M. Nieminen, Phys. Rev. B 58 (1988) 14 288.
[21] H.J. Jensen, Self-Organized Criticality, Cambridge University Press, Cambridge, 1998, and references therein.
[22] G. Caldarelli, C. Castellanos, A. Petri, Physica A 270 (1999) 15.
[23] T.E. Harris, The Theory of Branching Processes, Springer, Berlin, 1963.
[24] O. Sotolongo-Costa, Y. Morena, J.J. Llovera, J.C. Antoranz, Phys. Rev. Lett. 76 (1996) 42.
[25] J.B. Gómez, D. Iñiguez, A.F. Pacheco, Phys. Rev. Lett. 71 (1993) 380.
[26] B.Q. Wu, P.L. Leath, Phys. Rev. B 59 (1999) 4002.
[27] J. Cardy, Scaling and Renormalization in Statistical Physics, Cambridge Lectures Notes in Physics 5, Cambridge, 1996.
[28] L. Monette, Int. J. Mod. Phys. B 8 (1994) 1417.
[29] P.C. Hemmer, A. Hansen, J. Appl. Mech. 59 (1992) 909.
[30] M. Kloster, A. Hansen, P.C. Hemmer, Phys. Rev. E 56 (1997) 2615.
[31] D. Sornette, J. Phys. A 22 (1989) L243.
[32] D. Sornette, J. Phys. I (France) 2 (1992) 2089.
[33] D. Sornette, J.V. Andersen, Eur. Phys. J. B 1 (1998) 353.